TISSUE ENGINEERING: Part A
Volume 25, Numbers 9 and 10, 2019

DOI: 10.1089/ten.tea.2018.0377

termis
Tissue Engineering
& Regenerative Medicine
International Society

2018 MARY ANN LIEBERT, INC. OUTSTANDING STUDENT AWARD OF TISSUE ENGINEERING AND REGENERATIVE MEDICINE INTERNATIONAL SOCIETY–AMERICAS

4-Hydroxybutyrate Promotes Endogenous Antimicrobial Peptide Expression in Macrophages

Catalina Pineda Molina, PhD,[1,2] George S. Hussey, PhD,[1,3] Jonas Eriksson, PhD,[1,3] Michael A. Shulock, BSc,[1,2] Laura L. Cárdenas Bonilla, BSc,[1] Ross M. Giglio, BSc,[1,2] Riddhi M. Gandhi, BSc,[1,2] Brian M. Sicari, PhD,[1,3] Derek Wang, BSc,[1] Ricardo Londono, PhD, MD,[1] Denver M. Faulk, PhD,[1,2] Neill J. Turner, PhD,[1,3] and Stephen F. Badylak, DVM, PhD, MD[1–3]

Naturally occurring antimicrobial peptides (AMPs) are effector molecules secreted by several cell types but especially by cells of the innate immune system such as macrophages. AMPs largely avoid resistance acquired by bacteria to man-made antibiotics. Different short chain fatty acids (SCFAs) have proven to be efficient inducers of AMP secretion. The SCFA butyrate is an endogenous histone deacetylase inhibitor that has been shown to induce the expression of the AMP *cramp* (cathelicidin LL-37) in cells of the immune system and mucosal epithelium, which provides protection against pathogens. Clinical applications of butyrate, however, are limited due to its cytotoxic effects. Hydroxylated derivatives of butyrate (2-hydroxybutyrate [2HB], 3-hydroxybutyrate [3HB], and 4-hydroxybutyrate [4HB]) are also endogenous molecules, but their capability of inducing AMP expression has been unexplored. 4HB has been used for the production of polymeric surgical meshes intended for soft tissue repair. This study evaluated the ability of hydroxylated derivatives of butyrate to induce the upregulation of AMPs in murine bone marrow-derived macrophages *in vitro*. Noncytotoxic effects and increased *cramp* and *β-defensin-4* were found to be induced by 4HB. An *in vivo* increased resistance to deliberate bacterial contamination was shown by a surgical mesh composed of a polymer of 4HB compared with polypropylene surgical mesh.

Keywords: antimicrobial peptides, histone deacetylase inhibition, short chain fatty acids, sodium butyrate, 2-hydroxybutyrate, 3-hydroxybutyrate, 4-hydroxybutyrate

Impact Statement

This study evaluated the biological activity of hydroxylated derivatives of butyrate as inductors of antimicrobial peptides (AMPs) in murine bone marrow-derived macrophages *in vitro*. A differential modulation of AMP expression by the hydroxylated derivatives of butyrate is shown. The ability of sodium 4-hydroxybutyrate to upregulate AMP expression through a histone deacetylase inhibitory-independent mechanism, and to promote increased resistance to bacterial contamination *in vivo* are also shown. The findings provide an alternative for prevention of bacterial contamination of implanted biomaterials. Functionalization of biomaterials with hydroxylated derivatives of butyrate can enhance the endogenous antimicrobial activity of the immune system through increased production of AMPs by host cells, thus providing protection against bacterial contamination.

Introduction

Biomaterial-associated infections and the emergence of antibiotic-resistant bacteria represent significant challenges for surgeons and the field of biomaterials, in general. Surgical site infections are considered the main cause of implant failure,[1] with an incidence as high as 33%.[2] Current strategies to prevent such infections are only marginally effective, especially with respect to biofilm formation. Moreover, the indiscriminate use of antibiotics and the suboptimal concentrations of antibiotics used when administered within the wound site or as coating for biomaterials can actually promote biofilm formation and an increased resistance to the antimicrobial agents.[3,4]

Antimicrobial peptides (AMPs) have long been recognized as part of the innate immune system defense against pathogens. AMPs can be effective even when bacteria are in a quiescent stage within a protective biofilm, providing an

[1]McGowan Institute for Regenerative Medicine, University of Pittsburgh, Pittsburgh, Pennsylvania.
Departments of [2]Bioengineering and [3]Surgery, University of Pittsburgh, Pittsburgh, Pennsylvania.

advantage over most current antibiotic agents,[4] and can prevent bacterial-associated biofilm formation[5] and persistent infection.[6,7]

The major groups of AMPs in mammals are defensins, cathelicidins, and histatins.[8] The mechanisms of action of AMPs include their ability to interact with negatively charged bacterial membranes because of their cationic polarity, and promote disruption and permeabilization of the bacterial membrane. AMPs can also target and block specific molecules of bacterial metabolic pathways.[5] Various AMPs have been shown to downregulate the gene expression of molecules required for bacterial motility and matrix synthesis through inhibition of transcriptional activators of the quorum-sensing systems and the intracellular stringent response signal (p)ppGpp, affecting bacterial communication within the biofilm.[4]

The functions of AMPs extend beyond antimicrobial activity. For example, defensins and cathelicidins are chemoattractants for immune cells to enhance the host response to bacterial contamination or infection.[9,10] The role of cathelicidin LL-37, the only human cathelicidin, in wound healing[11–13] and angiogenesis[14] has been recognized. Cathelicidin LL-37 is also implicated in a seemingly paradoxical response, since it promotes the expression of anti-inflammatory cytokines in already activated proinflammatory immune cells, acting as a modulator of the immune response and promoting local tissue homeostasis.[9]

Short chain fatty acids (SCFAs) are endogenous molecules with distinctive structural and functional activities. Butyrate represents one of the most abundant SCFAs produced by commensal microbiota in the gastrointestinal tract,[15] and promotes tissue homeostasis through its activity as a histone deacetylase (HDAC) inhibitor,[16] with associated immunomodulatory functions[17] and increased secretion of AMPs.[18] Hydroxylated derivatives of butyrate, namely 2-hydroxybutyrate (2HB), 3-hydroxybutyrate (3HB), and 4-hydroxybutyrate (4HB), are endogenous metabolites in other tissues.[19–22]

In particular, 4HB has been exhaustively studied for its role as modulator of the neurotransmitter γ-aminobutyric acid (GABA) in the central nervous system (CNS),[20] and for its protective effects against stress and ischemia.[23] Moreover, 3HB and 4HB have been used for the production of polymeric mesh materials for soft tissue repair and regenerative medicine applications.[24,25] The potential of hydroxylated forms of butyrate to control bacterial infections through promotion of endogenous upregulation of AMPs, however, remains unknown.

The objectives of this study were to characterize the expression of AMPs in murine bone marrow-derived macrophages stimulated with hydroxylated forms of butyrate *in vitro,* and whether the AMP induction involved changes in the HDAC activity. The ability of a 4HB polymer to resist bacterial contamination *in vivo* was also investigated.

Materials and Methods

Monomers

Sodium butyrate (Cat. No. B5887; Sigma), butyric acid (Cat. No. B103500; Sigma), sodium 2-hydroxybutyrate (Na-2HB, Cat. No. 220116; Sigma), 2-hydroxybutanoic acid (Acid-2HB, Cat. No. CDS000492; Sigma), sodium 3-hydroxybutyrate (Na-3HB, 54965; Sigma), 3-hydroxybutyric acid (Acid-3HB, Cat. No. 166898; Sigma), and sodium 4-hydroxybutyrate (Na-4HB, G-001; Sigma) were used in this study (Supplementary Fig. S1). The methanol containing the Na-4HB was evaporated at room temperature and the Na-4HB was further solubilized in sterile type I water. Only a sodium salt form of 4HB (Na-4HB) was included in the study. The monomer 4-hydroxybutyric acid is a controlled substance and not commercially available and, therefore, was not evaluated herein.

Overview of experimental design

In vitro study. The effects of acid and sodium salt forms of butyrate and its hydroxylated derivatives upon HDAC activity and the expression of the AMP *cramp* (cathelicidin LL-37), and *β-defensins 2, 3,* and *4* in murine bone marrow-derived macrophages were determined. A dose–response curve was established for each SCFA to determine effects upon cell viability and the levels of expression of AMPs (Fig. 1A).

In vivo studies. A rat model of an abdominal wall partial thickness defect[26,27] (Fig. 1B) and a rat model of deliberate contamination in a subcutaneous tissue pocket[28] (Fig. 1C) were used to evaluate the expression of *cramp* (cathelicidin LL-37) in the presence of sterilized P4HB (poly 4-hydroxybutyrate) surgical mesh and contaminated surgical mesh, respectively.

Isolation and culture of murine bone marrow-derived macrophages

Bone marrow-derived monocytes were obtained from female C57bl/6 mice (Jackson Laboratories, Bar Harbor, ME) and differentiated into macrophages as previously described.[29,30] In brief, animals were euthanized by CO_2 inhalation and subsequent cervical dislocation in accordance with the guidelines of the American Veterinary Medical Association (AVMA) Panel of Euthanasia. After euthanasia and using an aseptic technique, the skin of the inferior legs was completely removed, the coxa-femoral joint was disarticulated, and the legs harvested. The excess of muscle was removed, and after disarticulation of tarsus and stifle, tibia and femoral bones were isolated. Under sterile conditions, the ends of each bone were transected and the bone marrow flushed with medium using a 30G needle.

Harvested monocytes were seeded at a ratio of 2×10^6 cells/mL and differentiated into macrophages by culture for 7 days with macrophage colony-stimulating factor-containing media (Dulbecco's modified Eagle's medium high glucose [Gibco, Grand Island, NY], supplemented with 10% fetal bovine serum [Invitrogen, Carlsbad, CA], 10% L929 cell conditioned media, 50 μM beta-mercaptoethanol [Gibco], 100 U/mL penicillin, 100 μg/mL streptomycin, 10 mM nonessential amino acids [Gibco], and 10 mM hepes buffer). Cells were maintained at 37°C and 5% CO_2 with media changes every 48 h. All procedures were approved by and performed according to the guidelines of the Institutional Animal Care and Use Committee at the University of Pittsburgh (IACUC protocol #15086460).

Stimulation of macrophages with butyrate or its hydroxylated derivatives

Naive macrophages were stimulated with a series of increasing concentrations (as specified for each experiment) of acid or sodium salt forms of butyrate or its hydroxylated derivatives (2HB, 3HB, and 4HB) for 24 h at 37°C, 5% CO_2.

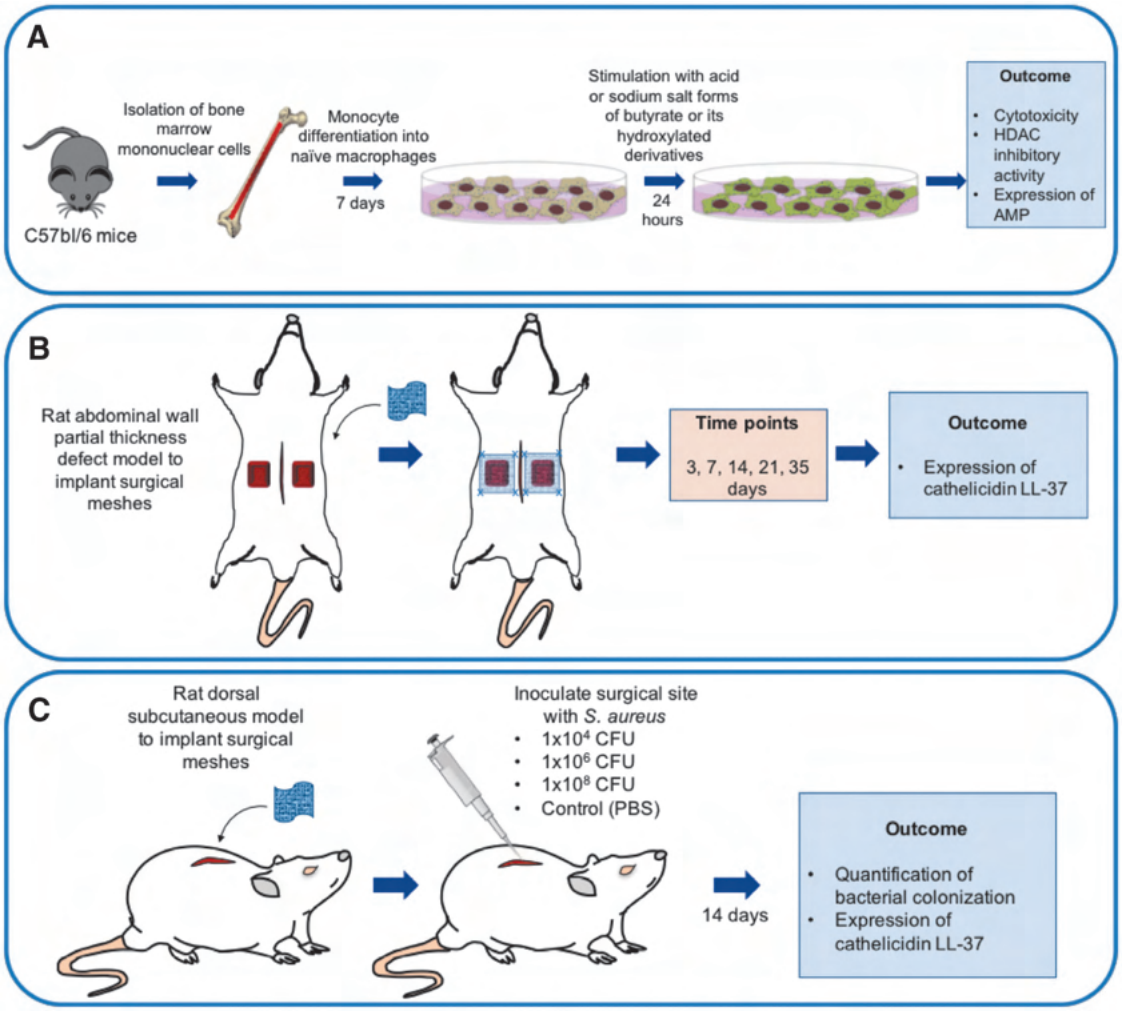

FIG. 1. Experimental design overview. **(A)** *In vitro* effects of acids and sodium salt forms of butyrate or its hydroxylated derivatives upon macrophages. Primary macrophages were differentiated from mononuclear cells harvested from the bone marrow of C57bl/6 mice and exposed to a dose–response of each of the SCFA for 24 h. The cytotoxicity induced by the SCFA was evaluated with MTT and LIVE/DEAD assays. The ability of the SCFA to induce the expression of the AMP *cramp* (cathelicidin LL-37), and *β-defensins 2, 3,* and *4* was investigated. Finally, their activity as HDAC inhibitors at a concentration found to induce AMP expression in macrophages was determined. **(B)** *In vivo* secretion of cathelicidin LL-37 induced by an exogenous source of 4HB. Expression of cathelicidin LL-37 around surgical meshes of P4HB (Phasix™ Mesh; C.R. BARD, Warwick, RI) and PP (Bard® Mesh; C.R. BARD) was evaluated in a Sprague Dawley rat partial thickness abdominal wall defect model. A 1.5×1.5 cm test article was implanted after surgical removal of the external and internal oblique muscles. Defect only was used as a control. The animals were sacrificed and materials harvested at 3, 7, 14, 21, and 35 days postsurgery. Explanted specimens were used for immunolabeling using an antibody specific for cathelicidin LL-37. **(C)** A rat dorsal subcutaneous model was used to study the resistance to bacterial contamination of surgical meshes composed of P4HB and PP. After implantation, one of three different concentrations of a clinical isolate of *Staphylococcus aureus* was inoculated on the mesh material, or PBS was used as negative control. Sham-operated animals without mesh were used as a second control. The test devices were explanted after 14 days. The number of bacteria colonizing the meshes was quantified. AMPs, antimicrobial peptides; HDAC, histone deacetylase; MTT, 3-(4,5-dimethythiazol-2-yl)-2,5-diphenyltetrazolium bromide; P4HB, poly 4-hydroxybutyrate; PBS, phosphate-buffered saline; PP, polypropylene; SCFAs, short chain fatty acids.

Macrophage metabolism and cell viability

Metabolism and viability of stimulated macrophages were measured using the MTT [3-(4,5-dimethythiazol-2-yl)-2,5-diphenyltetrazolium bromide] assay (Vibrant® MTT Cell Proliferation Assay Kit, V-13154; Molecular Probes) following the manufacturer's instructions. In brief, 1×10^5 bone marrow-derived monocytes were plated and differentiated into macrophages as described earlier. Each of the SCFA was evaluated at 0.05, 0.1, 0.25, 0.5, 1, 2, 4, 12, 24, and 48 mM for 24 h at 37°C, 5% CO_2.

After stimulation, macrophages were washed with phosphate-buffered saline (PBS) and incubated with 100 μL of serum- and antibiotic-free media containing 1.2 mM MTT solution for 2 h. After the incubation period, 75 μL of media was removed from each well and the formazan produced by reduction of the MTT was diluted with 50 μL of dimethyl sulfoxide. After an incubation period of 10 min at 37°C, the

concentration of formazan was determined by optical density at 540 nm. The metabolic activity of macrophages was calculated from a standard curve. Results were presented relative to untreated (media only) macrophages.

Viability of treated macrophages was also evaluated using a two-color fluorescent cell viability assay (LIVE/DEAD™ Cell Imaging Kit [488/570], R37601; Invitrogen™ Molecular Probes™) following manufacturer's instructions. In brief, 1×10^6 bone marrow-derived monocytes were differentiated into macrophages. Each of the SCFA was evaluated at 0.05, 0.1, 0.25, 0.5, 1, 2, 4, 12, 24, and 48 mM for 24 h at 37°C, 5% CO_2. After the incubation period, a solution containing fluorochromes for live cells (green) and dead cells (red) was added to the cells, and incubated for 15 min at room temperature. Images of three 20× fields were immediately taken for each well using a live-cell microscope using FITC (green) and 594 (red) filters.

Immunolabeling for cathelicidin LL-37

To determine whether the SCFA have an effect on the expression of the AMP cathelicidin LL-37, murine bone marrow-derived macrophages (2×10^6 cells) were stimulated with several noncytotoxic concentrations of acid or sodium salt forms of butyrate (0.05, 0.1, 0.25, 0.5, 1, or 2 mM) or its hydroxylated derivatives (2HB, 3HB, and 4HB) (0.05, 0.1, 0.25, 0.5, 1, 2, 4, or 12 mM) for 24 h. Treated macrophages were fixed in 2% paraformaldehyde for 30 min, followed by washes with PBS. Fixed cells were then incubated for 1 h with blocking buffer (4%v/v horse serum, 2%w/v bovine serum albumin, 0.1%v/v triton X-100, and 0.1%v/v tween-20 in PBS) to inhibit nonspecific binding of antibodies.

After blocking, macrophages were incubated with the primary rabbit polyclonal antibody cathelicidin LL-37 (Cat. No. 253814; Abbiotec) at 1:100 dilution at 4°C overnight. After washing in PBS, the macrophages were incubated with fluorophore-conjugated secondary antibody, goat anti-rabbit Alexa Fluor 488 (Cat. No. A11034; Invitrogen) at 1:200 dilution for 1 h at room temperature. After washing again with PBS, nuclei were counterstained with 4′,6-diamidino-2-phenylindole (DAPI) before imaging. Images of three 20× fields were taken for each well using a live-cell microscope.

Gene expression of AMPs

Sodium salt forms of butyrate (0.5–2 mM) or its hydroxylated derivatives (Na-2HB, Na-3HB, and Na-4HB) (0.5–4 mM) were used to quantify transcription of AMP mRNAs. Total RNA was extracted from 4×10^6 stimulated macrophages with 800 μL TRIzol reagent (Cat. No. 15596018; Ambion). The solution was mixed with 200 μL chloroform, vortexed for 15 s and centrifuged at 12,000 *g* for 10 min. The aqueous phase was transferred to a new tube and the RNA precipitated with 3 M sodium acetate (1/10 of the volume) and isopropanol (1 volume), followed by centrifugation at 18,000 *g* for 20 min. RNA purification was accomplished by washing the RNA pellet in 75% ethanol with an additional centrifugation at 18,000 *g* for 15 min. The RNA pellet was air dried and resuspended in nuclease-free water.

One microgram RNA was converted into cDNA using the High Capacity cDNA Reverse Transcription Kit (Cat. No. 4368814; Invitrogen) following manufacturer's instructions. Real-time quantitative polymerase chain reaction (qPCR) was performed using PowerUp™ SYBR® Green Master Mix (Cat. No. A25778; Applied Biosystems) to determine the levels of expression of the AMP cathelicidin LL-37 (*cramp*)[31] and *β-defensins 2, 3*, and *4*.[32] The levels of expression were normalized with the housekeeping gene *hprt1*[33] (Supplementary Table S1). Results are expressed as relative fold change log ($2^{-\Delta\Delta Ct}$) relative to nontreated macrophages.

HDAC inhibitory activity

To determine if the driving mechanism inducing the expression of AMPs in macrophages stimulated with the sodium forms of butyrate or its hydroxylated derivatives (Na-2HB, Na-3HB, and Na-4HB) involved the direct inhibition of the enzymatic activity of HDAC, an HDAC inhibitory assay was conducted. For each of the evaluated monomers, a single concentration identified to induce the expression of AMP was selected.

Murine bone marrow-derived macrophages (4×10^6 cells) were treated with 1 mM sodium butyrate, 4 mM of each of the sodium hydroxylated derivatives (Na-2HB, Na-3HB, Na-4HB), or the controls 0.375 μM trichostatin A (TSA; AAT Bioquest®, Inc), 6.25 or 12.5 μM histone acetyl transferase inhibitor (Cat No. S7152; Selleckchem) for 24 h, followed by evaluation of the HDAC activity. The results were compared with the levels of acetylation of the histone H3 by western blot using the specific antibody anti-Histone H3 (acetyl K9) (Cat No. ab61231; Abcam).

In addition, the HDAC activity of naive macrophage protein extracts was evaluated at a series of concentrations (0.5–96 mM) of each of the sodium forms of butyrate or the hydroxylated derivatives (Na-2HB, Na-3HB, and Na-4HB) to determine whether other concentrations were associated with inhibitory activity. The dose–response study was conducted following manufacturer's instructions. In brief, 5 μg of total protein extracts were incubated for 20 min at 37°C with increasing concentrations of each of the SCFA. A series of increasing concentrations of sodium butyrate and 3 μM TSA were used as controls.

Total protein isolation. Murine bone marrow-derived macrophages (4×10^6 cells) were harvested using a cell scraper. After centrifugation at 3500 *g* for 5 min at 4 C, supernatants were removed and the cells were washed twice with 1000 μL PBS. The cells were then lysed with lysis buffer (150 mM NaCl, 50 mM Tris pH 8.0, 1%v/v Triton X-100, 0.5%v/v sodium deoxycholate, 0.1%wt/v sodium dodecyl sulfate [SDS] and protease and phosphatase inhibitor cocktail [Cat No. PIA32961; Thermo Fisher Scientific]), incubating on ice for 1 h, and vortexing for 30 s every 10 min. After incubation, the lysis solution was centrifuged at 14,000 *g* for 15 min, and the supernatant containing the proteins was transferred to a new tube. The concentration of protein was quantified using the Pierce™ BCA Protein Assay Kit (Cat No. 23225; Thermo Fisher Scientific), following manufacturer's instructions.

HDAC activity. The Amplite™ Fluorimetric HDAC activity Assay kit *Green Fluorescence* (Cat No. NC1484042; AAT Bioquest) was used following the manufacturer's instructions. To determine the HDAC activity,

50 μL of HDAC Green™ Substrate working solution was added to the protein extracts and incubated for 1 h at 37 C. Fluorescence intensity was read at Ex/Em = 490/525 nm. Percentage of HDAC inhibition was calculated relative to the noninhibited control.

In vivo *expression of cathelicidin LL-37 induced by an exogenous source of 4HB*

The expression of cathelicidin LL-37 induced by implanted P4HB mesh (Phasix™ Mesh; C.R. BARD, Warwick, RI) or polypropylene (PP) mesh (Bard® Mesh; C.R. BARD) was evaluated using a rat model of abdominal wall bilateral partial thickness defect.[26,27] A defect without implant was used as a control (Fig. 1B). Animal procedures were approved by and performed according to the guidelines of the Institutional Animal Care and Use Committee at the University of Pittsburgh (IACUC protocol #15127009). Thirty Sprague Dawley rats were randomly divided into three separate equal groups of 10.

Each rat was anesthetized and maintained at a surgical plane of anesthesia with 2% isoflurane in oxygen. The surgical site was prepared in sterile manner using a betadine (povidone-iodine) solution followed by placement of sterile drapes. Bilateral paramedian skin incisions were made to provide access to the muscular abdominal wall. Partial thickness defects measuring 1 × 1 cm were created in the exposed musculature by removing the external and internal oblique muscles on each side of the midline, leaving the underlying peritoneum and transversalis fascia intact.

The two defects on each animal were then either repaired with one of the test articles or left unrepaired ($N = 4$ biological replicates for each group at each time point). Each mesh was sutured to the adjacent abdominal wall musculature with 4-0 Prolene nonabsorbable suture at each corner to secure the mesh and allow for partial mechanical loading of the test article, and to allow for identification of the implant boundaries at the time of euthanasia and explanation. The skin was closed using absorbable 4-0 Vicryl™ suture. The animals were recovered from anesthesia on a heating pad and allowed normal activity and diet for the remainder of the study period.

Test article collection. At 3, 7, 14, 21, and 35 days postimplantation, two animals in each group were euthanized by CO_2 inhalation and subsequent cervical dislocation in accordance with the guidelines of the AVMA Panel of Euthanasia. After euthanasia and using sterile technique, the skin was gently dissected and reflected, and the test specimens and surrounding tissue were collected and immersed in 10% neutral buffered formalin for subsequent histological evaluation.

Immunolabeling of tissue sections. Cells expressing *cramp* (cathelicidin LL-37) within each field of view, at the mesh–tissue interface, were identified and quantified by immunofluorescence. Antigen retrieval of tissue sections was facilitated with citrate buffer (10 mM citrate, pH 6.0) at 95–100°C for 20 min. The blocking solution was applied for 1 h followed by the same staining procedure described in the *in vitro* Immunolabeling for Cathelicidin LL-37 section. Four multispectral epifluorescent images were acquired for each slide at the mesh–tissue interface (Nuance multispectral imaging system; CRi, Inc.). The total number of cells expressing *cramp* (cathelicidin LL-37) was quantified for each image using CellProfiler Image Analysis Software.

Resistance of implanted surgical meshes to deliberate bacterial contamination

The ability of implanted P4HB mesh to resist contamination with one of three different concentrations of *Staphylococcus aureus* was evaluated in a rat model of subcutaneous tissue pocket[28] (Fig. 1C).

Preparation of bacterial inoculum. Single colonies of a clinical isolate *S. aureus* (ATCC 25923) were cultured in tryptic soy broth (Soybean-Casein Digest Medium; BD) overnight at 37°C with constant shaking. *S. aureus* concentration was calculated based on optical density and compared with a predetermined growth curve for the bacterial strain. 1×10^4 CFU, 1×10^6 CFU, or 1×10^8 CFU *S. aureus* were obtained by diluting the cultured bacteria to a final volume of 100 μL in sterile PBS.

Bacterial inoculation upon implanted mesh materials. All procedures were approved by and performed according to the guidelines of the Institutional Animal Care and Use Committee at the University of Pittsburgh (IACUC protocol #14020360). Seventy-two Sprague Dawley rats were randomly divided into three equal groups of 24. Anesthesia was induced with 2.5–4% isoflurane, and surgical plane anesthesia was maintained with 0.5–4% isoflurane throughout the procedure. The surgical site was prepared by clipping the fur over the entire dorsal region, and cleaning the operative site with three alternating scrubs of povidone-iodine surgical scrub and 70% isopropyl alcohol solutions. A final scrub with 70% isopropyl alcohol was applied and allowed to dry, followed by placement of sterile surgical drape(s) over the entire field.

A 1 cm incision was made over the dorsal midline and a 2.0 × 3.0 cm subcutaneous pocket was created on one side of the midline. Each animal received one sterile 2.0 × 3.0 cm test article (P4HB or PP) implanted into the dorsal subcutaneous pocket. In brief, the surgical mesh device was folded over itself to minimize contact with the skin during the implantation. Once positioned in the pocket, the test article was unfolded. After implantation, the surgical site was inoculated with one of the *S. aureus* preparations: 1.0×10^4 CFU, 1.0×10^6 CFU, or 1.0×10^8 CFU in 100 μL sterile PBS, designated as low, medium, and high inoculation levels, respectively. Noncontaminated test articles were injected with 100 μL sterile PBS.

After placement of the test article and the designated inoculum ($N = 6$ devices per inoculation level), the skin was closed with a continuous 4-0 Vicryl suture. For the sham-operated group, the inoculum was injected into the dorsal subcutaneous pocket without any implanted material, followed by skin closure as described earlier. Each animal was recovered from anesthesia, returned to its cage, and allowed free access to food and water *ad libitum*. Rats were given Buprenex® (0.06 mg/kg subcutaneously) and Baytril® (5 mg orally) at the time of surgery and for 3 days postsurgery.

Test article collection. At 14 days postimplantation, six animals per group per inoculation level were euthanized by CO_2 inhalation and subsequent cervical dislocation in accordance with the guidelines of the AVMA Panel of Euthanasia. After euthanasia and using sterile technique, the skin was gently dissected and reflected, the specimens and surrounding tissue were collected. Using a sterile razor blade, 100 mg of the collected specimens were used for *S. aureus* quantification, as described hereunder.

Quantification of *S. aureus*. One hundred milligrams of the explanted specimen (mesh and adjacent tissue) were taken from the lateral edge near the center of the mesh, immersed in 5 mL sterile PBS, and homogenized for 30 s at room temperature to dissociate adherent bacteria. 1:1000 and 1:10,000 dilutions were prepared from the homogenized PBS solution. Undiluted and diluted solutions were plated on tryptic soy agar plates. The plates were incubated at 37°C for 24 h and *S. aureus* colonies quantified for each specimen.

Statistical analysis

Data are presented as the mean ± standard error of the mean. For both *in vitro* and *in vivo* studies, statistical differences were determined using a nonparametric ANOVA test (Kruskal–Wallis test). Differences were compared with *post hoc* Dunn's test relative to nontreated macrophages *in vitro* and between the implanted mesh materials *in vivo*. The fold change gene expression relative to nontreated macrophages was analyzed using the BootstRatio Web Application for the ratio between the treatments and the control.[34] A value $p < 0.05$ was considered statistically significant. Statistical analysis was performed using GraphPad Prism version 6.07 (GraphPad Software, La Jolla CA).

Results

Sodium hydroxylated derivatives of butyrate are not associated with a cytotoxic effect upon murine bone marrow-derived macrophages

The influence on macrophage metabolic activity and viability induced by sodium salt and acid forms of butyrate or its hydroxylated derivatives was determined. Exposure of murine bone marrow-derived macrophages to increasing concentrations of sodium butyrate, butyric acid, or the acid hydroxylated derivatives (acid-2HB and acid-3HB) induced a reduction in the cell metabolic activity by >50%, as shown by MTT assay (Fig. 2). Concentrations >2 mM of butyrate and butyric acid, and concentrations >24 mM of acid-2HB and acid-3HB were associated with a cytotoxic effect, as shown by MTT and LIVE/DEAD assays (Fig. 2 and Supplementary Fig. S2). In contrast, the sodium hydroxylated derivatives of butyrate (Na-2HB, Na-3HB, and Na-4HB) preserved the viability of stimulated macrophages at all tested concentrations.

Na-4HB induces an increased expression of the AMP cramp (cathelicidin LL-37) in stimulated murine bone marrow-derived macrophages

The effect of hydroxybutyrate isomers upon the endogenous expression of the AMP *cramp* (cathelicidin LL-37) in stimulated macrophages was evaluated and compared with the induction of cathelicidin LL-37 expression produced by sodium butyrate. All SCFAs induced a differential expression of cathelicidin LL-37 (Fig. 3A). Concentrations inducing a significantly higher production of cathelicidin LL-37 when compared with nontreated macrophages were 0.5 and 2 mM of sodium butyrate, 2 and 4 mM of Na-2HB, 2 mM of Na-3HB, and between 0.5 and 12 mM of Na-4HB (Fig. 3B). The acid counterparts of the evaluated SCFAs (butyric acid, acid-2HB, and acid-3HB) did not significantly induce the expression of cathelicidin LL-37 when compared with the nontreated macrophages (Fig. 3B).

Na-4HB induces a transcriptional activation of AMPs in exposed macrophages

Results from the immunolabeling of cathelicidin LL-37 were used as a reference to limit the monomers and concentrations required to determine the level of expression of the genes *cramp* (cathelicidin LL-37), and *β-defensins 2, 3*, and *4*. Acid forms of butyrate or its hydroxylated derivatives were excluded from this experiment since they were not associated with a significant increased expression of cathelicidin LL-37 at any of the evaluated concentrations (Fig. 3).

Murine bone marrow-derived macrophages exposed to the evaluated SCFAs were further evaluated by RT-qPCR to determine if the expression was associated to a transcriptional activation of the gene. Transcriptional activation of the genes codifying for *β-defensins 2, 3,* and *4* were also evaluated in treated macrophages. mRNA transcription of the genes was evaluated in macrophages exposed to sodium hydroxylated derivatives of butyrate (Na-2HB, Na-3HB, and Na-4HB) and compared with nontreated macrophages. A statistically significant upregulation of the *cramp* gene was found in macrophages treated with 2 mM Na-3HB (mean fold change: 10.62, p ratio = 0.0045), and in those treated with Na-4HB at 1 mM (mean fold change: 8.14, p ratio = 0.001) or 2 mM (mean fold change: 3.49, p ratio = 0.013) (Fig. 4A).

None of the evaluated concentrations of sodium butyrate or its hydroxylated derivatives (Na-2HB, Na-3HB, and Na-4HB) were found to significantly increase the transcription of *β-defensin 2* and *β-defensin 3* genes (Fig. 4B, C).

Transcriptional activation of the *β-defensin 4* gene was significantly induced by Na-4HB at both 2 mM (fold change: 2.73, p ratio = 0.018) and 4 mM (fold change: 3.00, p ratio = 0.024) (Fig. 4D).

AMP expression by macrophages stimulated with sodium butyrate and its hydroxylated derivatives and HDAC inhibitory activity

To determine if the AMP expression induced by macrophages treated with sodium forms of butyrate or its hydroxylated derivatives (Na-2HB, Na-3HB, and Na-4HB) was mediated by inhibition of HDAC activity, primary murine bone marrow-derived macrophages were tested with 1 mM sodium butyrate or 4 mM of each of the sodium hydroxylated derivatives (which were found to increase AMP expression on treated macrophages). No inhibition of HDAC activity was observed (Fig. 5A), suggesting that at least at these concentrations, the increased AMP expression is not due to a HDAC inhibitory activity. Western blot for acetyl-Histone 3, at the lysine 9 further confirmed that none of the treatments at the working concentrations had an effect upon the level of acetylation (Fig. 5B, C).

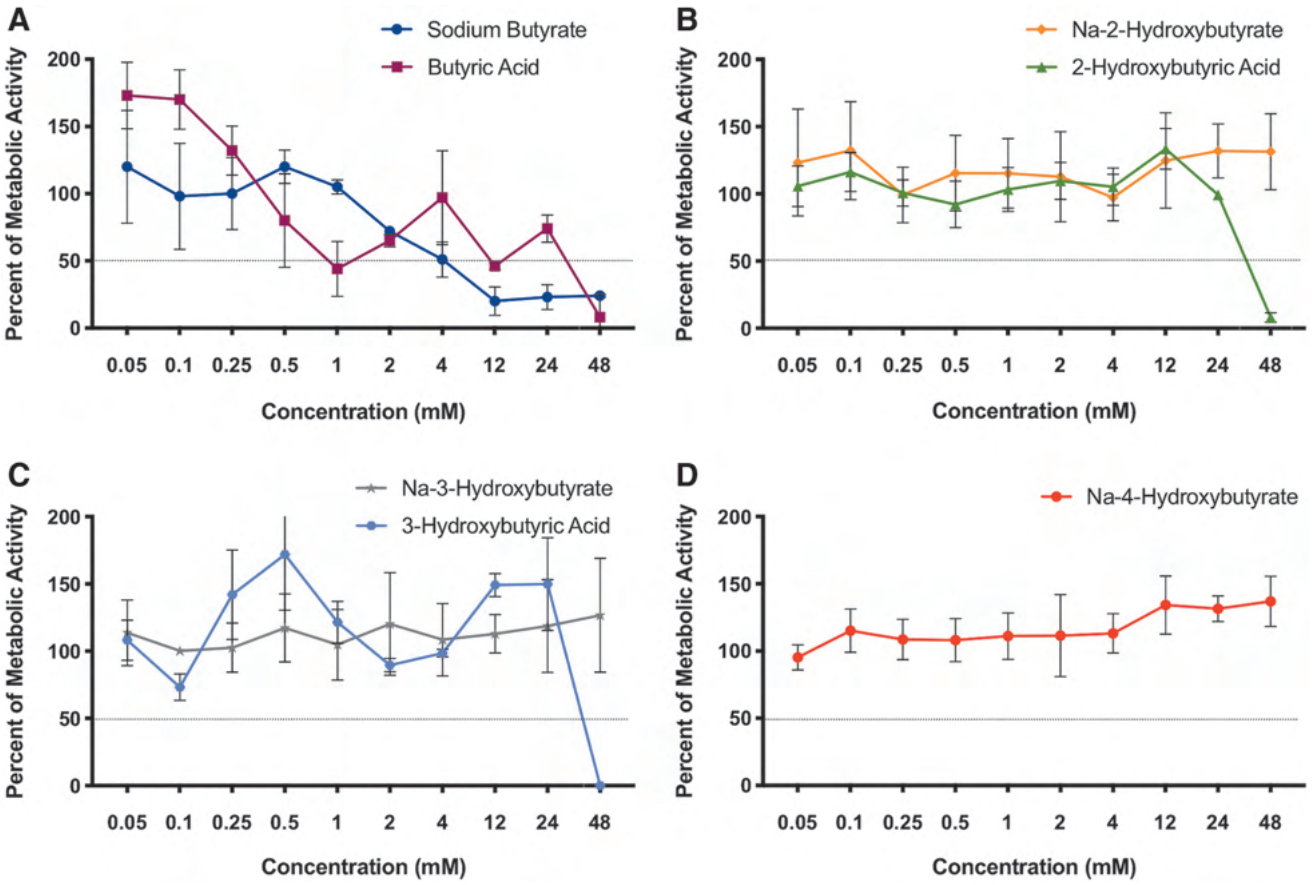

FIG. 2. Dose–response curves of butyrate and its hydroxylated derivatives. **(A)** Both sodium butyrate and butyric acid decreased the cell viability at concentrations >4 mM. **(B–D)** All hydroxylated forms of butyrate in their salt forms (Na-2HB, Na-3HB, and Na-4HB) are noncytotoxic at supraphysiological concentrations (48 mM). Acid forms of 2HB and 3HB decreased the cell viability at concentrations >24 mM. Value: mean ± SEM, $N = 3$ biological replicates, technical triplicates. 2HB, 2-hydroxybutyrate; 3HB, 3-hydroxybutyrate; 4HB, 4-hydroxybutyrate; Na, sodium; SEM, standard error of the mean.

Further, the ability of different concentrations of these SCFAs to inhibit HDAC enzymes in protein extracts was determined. There was a dose-dependent inhibition of HDAC activity by sodium butyrate and Na-2HB, but not with Na-3HB or Na-4HB (Fig. 5D). The half maximal inhibitory concentration (IC_{50}) was determined for sodium butyrate 3.69 ± 1.12 mM and for Na-2HB 12.51 ± 1.6 mM, using nonlinear fitting regression ($r^2 = 0.99$ and 0.96, respectively; GraphPad Prism). The dose–response results are consistent with the results obtained with the single doses used to treat the macrophages, which suggest that increases in the AMP expression are not due to a HDAC inhibitory activity of the used SCFAs.

In vivo *cramp (cathelicidin LL-37) expression increases around implanted surgical meshes after muscle injury*

Implanted P4HB or PP surgical meshes were used to evaluate and compare the expression of cathelicidin LL-37 in a rat model of abdominal wall partial thickness defect. Immunolabeling results showed an increase in the expression of *cramp* (cathelicidin LL-37) after muscle injury alone (without mesh placement) compared with noninjured muscle, as seen in the images of native muscle versus defect alone (Fig. 6A, B). Immunolabeling at the interface of the implanted surgical meshes showed an increased expression of *cramp* (cathelicidin LL-37) by the cells localized immediately around the fibers of P4HB and PP.

Quantification of the number of cells expressing cathelicidin LL-37 showed that P4HB was associated with the highest number of such cells around the mesh fiber at all time points, when compared with PP or the defect alone (Fig. 6B). Moreover, statistical analysis comparing the results among all the experimental groups at each time point showed that these numbers were significantly different when P4HB was compared with the defect alone at days 14 and 35, respectively, but only at 35 days when PP was compared with the defect alone. For all the evaluated time points, the number of cells expressing cathelicidin LL-37 was decreased in the native muscle group when compared with P4HB and PP, respectively.

P4HB surgical mesh is associated with resistance to deliberate bacterial contamination

A rat model of deliberate contamination in a subcutaneous tissue pocket was used to evaluate the resistance of P4HB surgical mesh to bacterial contamination. Quantification of bacteria within the explanted meshes at 14 days showed differences in the amount of viable *S. aureus* between the P4HB and PP (Fig. 7A). The noncontaminated

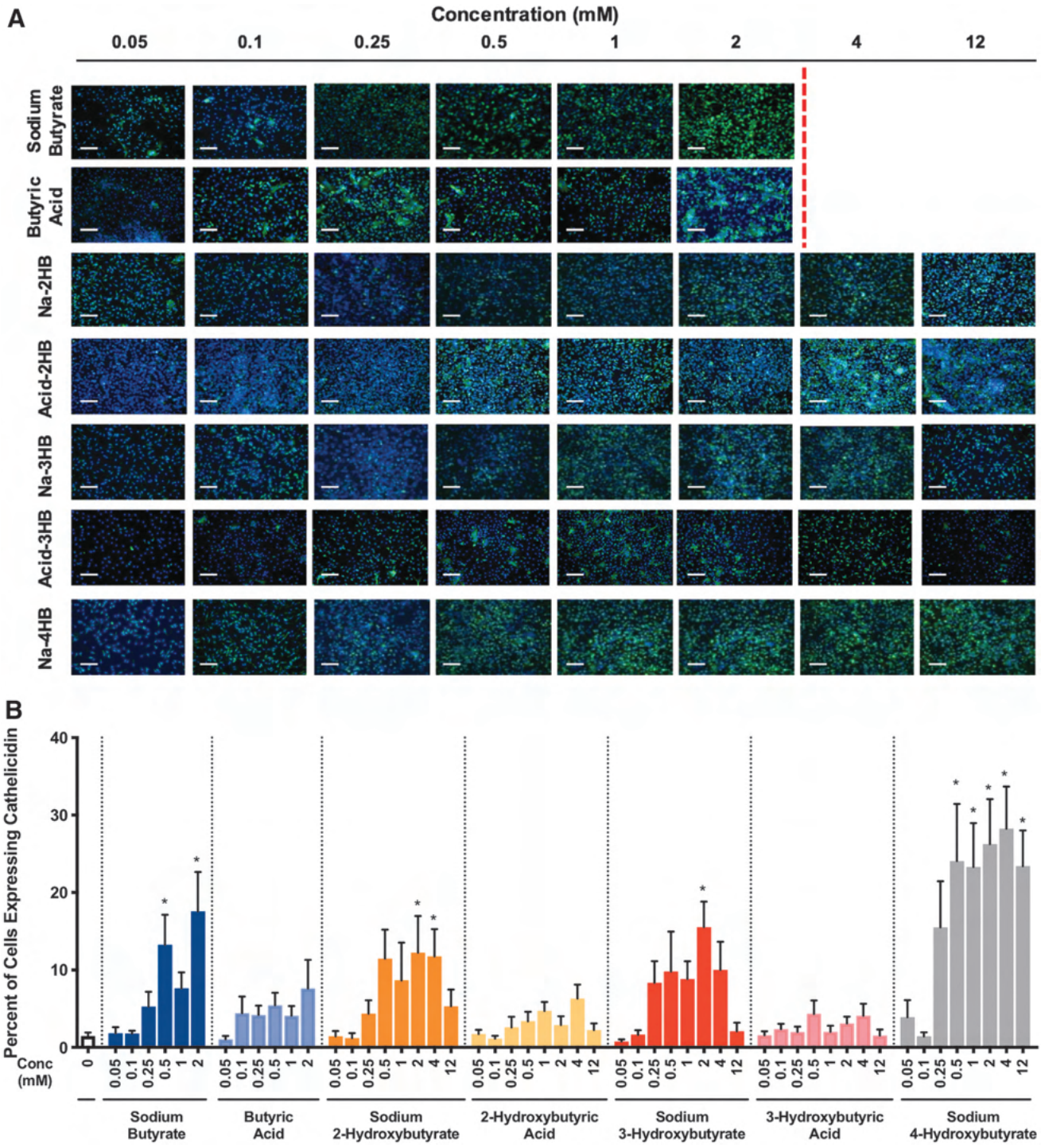

FIG. 3. Expression of cathelicidin LL-37 induced by butyrate and its hydroxylated derivatives. **(A)** Immunofluorescence for the AMP cathelicidin LL-37. A series of increased concentrations of acid and salt forms of butyrate or its hydroxylated derivatives were used to stimulate primary murine bone marrow-derived macrophages. Cathelicidin LL-37 positive expression is shown. Scale bar: 100 μm. $N = 3$ biological replicates, technical triplicates. **(B)** Quantification of cathelicidin LL-37 expression. Na-4HB induces the expression of cathelicidin LL-37 in amounts comparable with sodium butyrate. All hydroxylated forms have the ability to induce endogenous secretion of the AMPs, with higher levels in their sodium forms than in their acid forms. $^*p < 0.05$ relative to nontreated macrophages. Value: mean ± SEM, $N = 3$ biological replicates, technical triplicates.

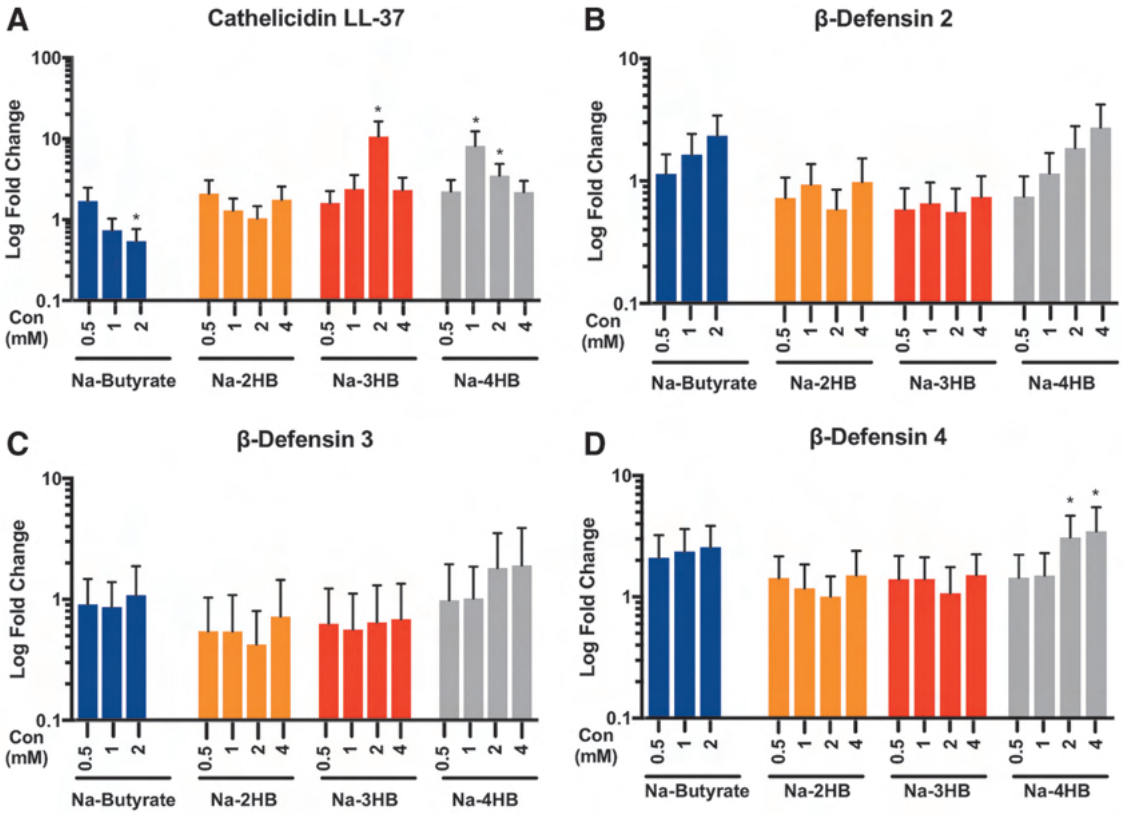

FIG. 4. Gene expression of AMPs induced by butyrate and its hydroxylated derivatives. **(A)** Na-3HB and Na-4HB induce an upregulation of the *cramp gene* at 1 and 2 mM compared with nontreated macrophages. **(B, C)** Expression of *β-Defensins* 2 and 3 are not significantly upregulated by any of the evaluated SCFA. **(D)** Na-4HB induce a significant transcriptional upregulation of *β-Defensin 4* at 2 and 4 mM compared with nontreated macrophages. Value: mean ± SEM, $N = 3$ biological replicates, technical triplicates.

controls had undetectable levels of bacterial contamination. For animals inoculated with a low level (1×10^4 CFU) of *S. aureus,* quantification of the recovered bacterial colonies showed $(5.5 \pm 3.4) \times 10^5$ CFU with PP $(7.2 \pm 7.1) \times 10^4$ CFU with P4HB, and $(1.2 \pm 1.0) \times 10^4$ CFU with the no-mesh control. Statistical analysis showed no differences in the recovered bacterial concentration among the groups at the low inoculation level.

At the medium (1×10^6 CFU) inoculation level, quantification of viable *S. aureus* showed $(1.6 \pm 1.2) \times 10^6$ CFU with PP $(1.8 \pm 0.2) \times 10^5$ CFU with the no-mesh control, and $(8.5 \pm 4.3) \times 10^4$ CFU with P4HB. Statistical analysis showed differences between the surgical meshes. PP showed amounts of *S. aureus* that were significantly higher than the number of colonies isolated from P4HB specimens ($p = 0.004$).

Data at the highest inoculation level (1×10^8 CFU) showed $(4.3 \pm 0.4) \times 10^6$ CFU with PP $(3.5 \pm 0.6) \times 10^6$ CFU with the no-mesh control, and $(1.3 \pm 0.7) \times 10^6$ CFU from P4HB. Analysis of the CFU counts at this level indicated that there were statistical differences between the surgical meshes. The number of *S. aureus* colonies isolated from PP were significantly higher than the number of colonies isolated from P4HB ($p = 0.015$).

Expression of cathelicidin LL-37 was evaluated in the contaminated field (Fig. 7B). Statistical analysis comparing the number of cells expressing cathelicidin Ll-37 between the evaluated groups at each inoculation level showed an increased expression around P4HB fibers compared with no mesh control at the no bacteria ($p = 0.0006$), low ($p = 0.024$), and medium ($p = 0.017$) inoculation levels (Fig. 7C). Statistical differences comparing the implanted meshes (P4HB vs. PP) were seen at the no bacterial control ($p = 0.001$).

Discussion

This study compared the effect of sodium butyrate and its hydroxylated derivatives (Na-2HB, Na-3HB, and Na-4HB) upon the expression of AMP and evaluated the HDAC activity of treated murine bone marrow-derived macrophages. The results showed that the hydroxylated derivatives of butyrate differentially modulate the macrophage expression of the AMP *cramp* (cathelicidin LL-37), and to a lesser degree the *β-defensin 4 in vitro*. Na-4HB induced the greatest level of endogenous expression of these AMPs; amounts comparable with those induced by sodium butyrate. Less induction of AMP expression was induced by Na-3HB, and the least by Na-2HB.

This study also showed preservation of cell viability when exposed to a wide range of physiological and supraphysiological concentrations of the hydroxylated derivatives of butyrate,[20,35] which contrasted with the cytotoxic effect induced by sodium butyrate.

Modulation of AMP can be epigenetically induced through the inhibition of HDAC enzymatic activity.[36] Different SCFAs have been associated with a weak HDAC inhibitory activity when compared with potent inhibitors such as TSA.[36] Variables such as concentration, cell type,

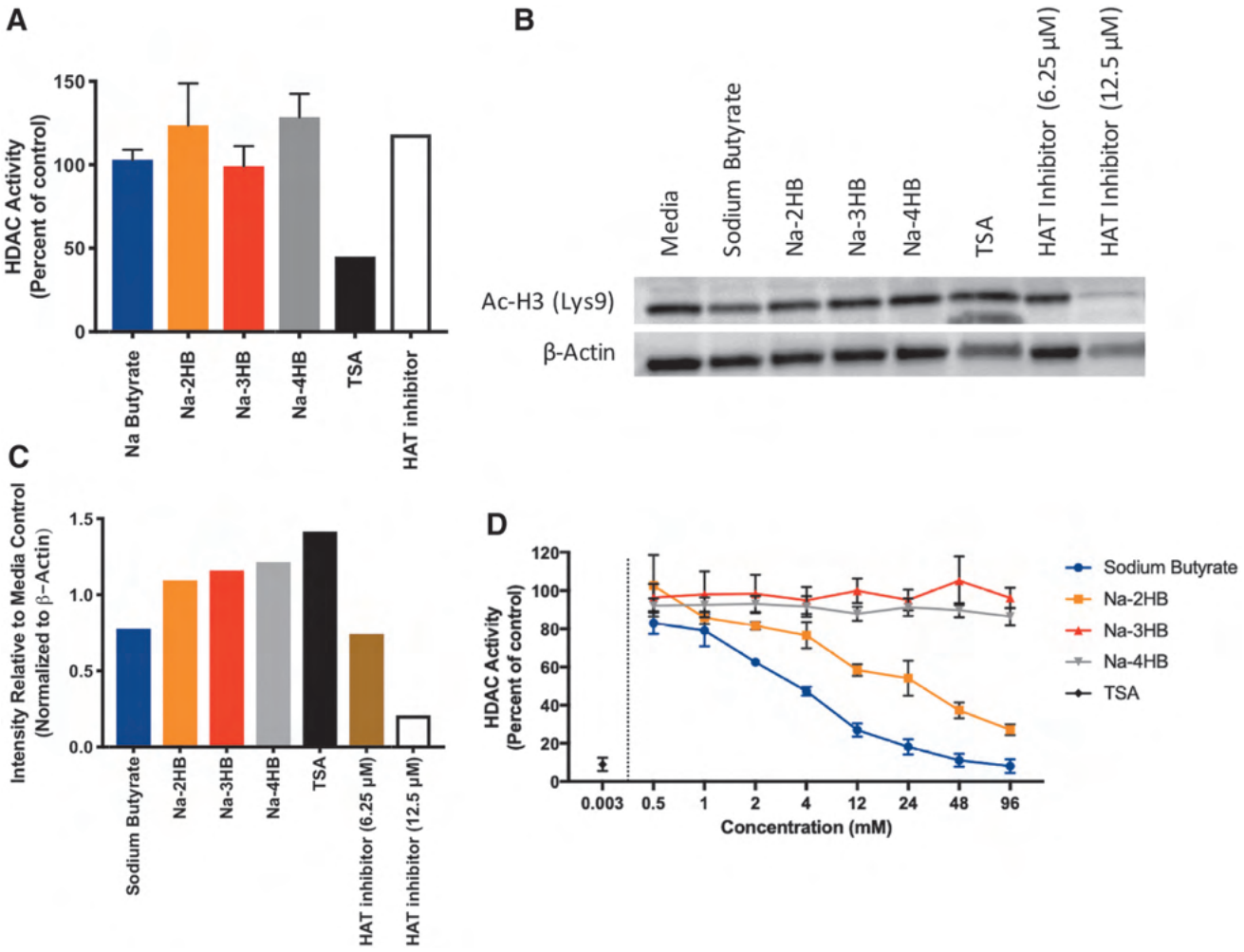

FIG. 5. Differential HDAC inhibition induced by sodium butyrate and its hydroxylated derivatives. **(A)** Murine bone marrow-derived macrophages were treated with 1 mM sodium butyrate or 4 mM of one of the hydroxylated derivatives (Na-2HB, Na-3HB, or Na4HB) for 24 h. Nontreated macrophages, 0.375 µM TSA, 6.25 or 12.5 µM HAT inhibitor were used as controls. HDAC activity of treated macrophages was determined and presented as a percentage normalized to nontreated macrophages. At the concentrations evaluated, none of the SCFA induced an HDAC inhibitory activity. **(B)** Representative western blot for acetyl (lys9)-histone 3, of three independent experiments. **(C)** Densitometry of western blot indicating the relative level of acetylation of histone 3 at the lysine 9 position. **(D)** HDAC activity in macrophage-derived protein extracts induced by increasing concentrations (0.5 to 96 mM) of sodium butyrate or each of the hydroxylated derivatives (Na-2HB, Na-3HB, and Na-4HB). 0.003 mM TSA or nontreated extracts were used as controls. HDAC activity is presented as a percentage normalized to nontreated protein extracts. A dose-dependent inhibition was found in protein extracts treated with sodium butyrate (IC_{50} 3.69 ± 1.12) mM and for Na-2HB (IC_{50} 12.51 ± 1.6), but not with Na-3HB and Na-4HB. HAT, histone acetyl transferase; TSA, trichostatin A.

specific HDAC groups and subgroups, and the ability of the molecule to enter into the nuclei, among others, are determinants in this activity.[37] Sodium butyrate is a known inhibitor of HDAC classes I and II in a broad spectrum of cell types. This molecule has been shown to induce apoptosis among different epigenetic effects.[38] Evaluation of sodium butyrate in this study confirms the HDAC inhibitory activity induced by this molecule in macrophage-derived protein extracts, and its cytotoxic effect when used at high concentrations.

This study also showed that the highest concentration found to increase the expression of AMP (4 mM) in macrophages stimulated with the hydroxylated derivatives of butyrate (Na-2HB, Na-3HB, and Na-4HB), was not associated with a HDAC inhibitory activity, suggesting that other mechanisms (e.g., direct signaling pathway regulation) may be involved in the gene expression of AMP. Additional evaluations of HDAC activity in macrophage-derived protein extracts with these hydroxylated derivatives showed distinct activity induced by Na-2HB compared with Na-3HB and Na-4HB, which warrants future studies using a broader spectrum of concentrations upon live macrophages.

Although the results of this study show that Na-2HB, Na-3HB, and Na-3HB did not have a HDAC inhibitory activity in treated macrophages at the evaluated concentration, these molecules have been clearly shown to inhibit HDAC activity in other body systems. For example, Shimazu *et al.*, showed that physiological circulatory concentrations of 3HB (>1 mM) during prolonged exercise or starvation have a direct HDAC inhibitory activity upon human embryonic kidney 293 (HEK293) cells *in vitro,* and whole kidney *in vivo,* in a dose-dependent

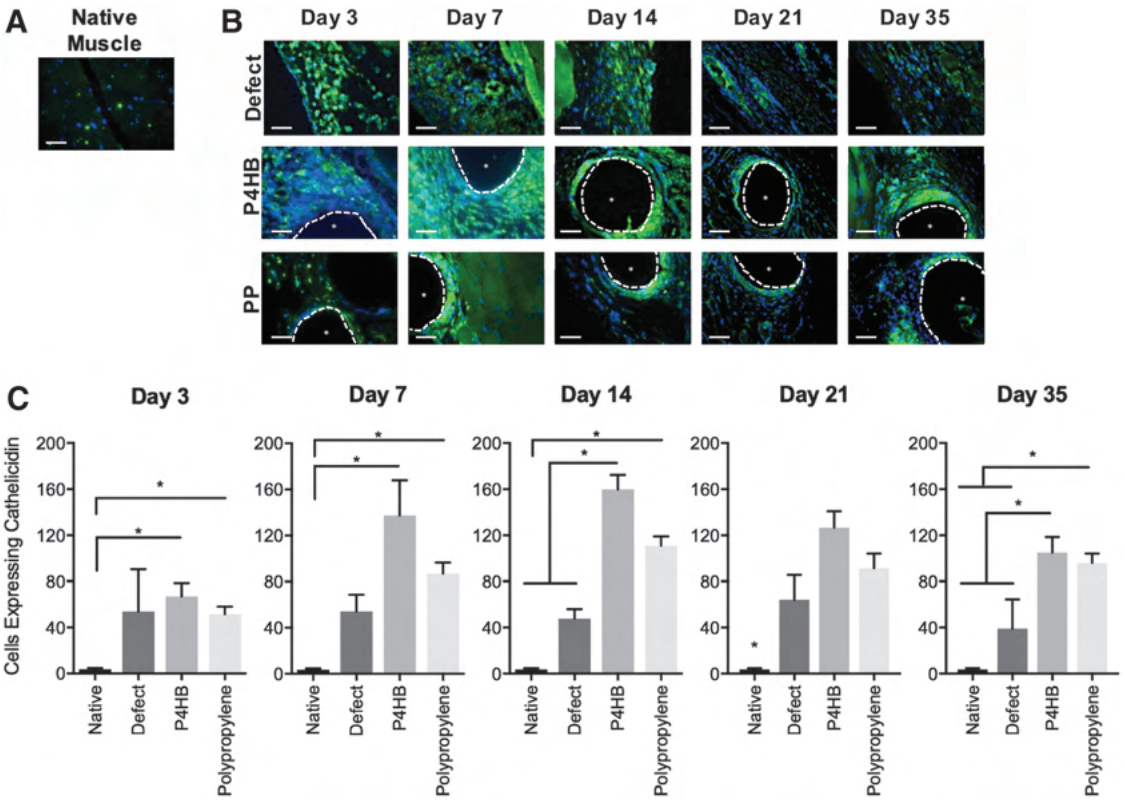

FIG. 6. *In vivo* expression of cathelicidin LL-37 around implanted P4HB and PP. **(A)** Basal expression of cathelicidin LL-37 in native muscle. **(B)** Immunolabeling of cathelicidin LL-37 surrounding the mesh fibers or the defect alone control. Increased expression of the antimicrobial peptide is associated with the tissue repair process, as evidenced in the defect alone samples. P4HB induces a higher level of expression compared with the defect alone. Fiber location is delineated by a *dotted line* and an *asterisk*. Scale bar 50 μm. **(C)** Quantification of cells expressing cathelicidin LL-37. Value: mean ± SEM, $N = 4$ biological replicates, technical triplicates, $^*p < 0.05$.

manner. The study reported that the major targets of acetylation were lysine 9 and 14 of histone 3, and that the inhibited HDAC belonged to classes I and II, with a generalized effect of protection against oxidative stress.[39]

Similarly, Klein *et al*. have shown a heterogeneous HDAC inhibitory response induced by 4HB in different regions of the rat brain. Whereas a significant acetylation was found in the cerebellum, the hippocampus, and brain stem, other regions such as the temporal and parietal cortex were shown to be unresponsive to 4HB. Of particular interest, only those regions that were responsive express class IV HDAC, suggesting that this subgroup is the target of 4HB.[40]

The lack of HDAC inhibitory activity associated with Na-4HB and its ability to upregulate the expression of AMP suggest a requirement for specific cell surface receptor triggering the transcriptional activation of AMP. It is hypothesized herein that the presence of the hydroxyl group at the carbons -2 and -3 diminishes the molecular interaction with the receptor, which results in a lower AMP induction. In fact, the presence of the 4-hydroxyl group has been shown to play a key role in high affinity interactions between 4HB and $GABA_A$ receptors in the brain.[41]

Other structural derivatives of butyrate, with chemical modifications in carbon-4, such as sodium 4-phenylbutyrate, have been shown to induce an effective transcriptional activation of AMP in epithelial cells and macrophages,[42–44] suggesting that functional modifications at this carbon level may not interfere with the molecular interactions, and thus have no detrimental effect upon AMP induction. The bioactivity of the 4-hydroxyl derivative, however, which is an endogenous metabolite of mammalian tissues,[40,41,45] has been less studied in tissues other than the CNS, and its potential to control bacterial infection through promotion of AMP has not been investigated. The increased expression of AMP as well as its ability to preserve cell viability suggest that Na-4HB may be used to functionalize biomaterials or as a cargo molecule for drug delivery, among others, without the risk of adverse effects.

This study showed the *in vivo* ability of a 4HB polymeric surgical mesh to resist different inoculation levels of bacterial contamination, which may be partially explained by the endogenous local induction of *cramp* (cathelicidin LL-37) expression. The results confirm the importance of *cramp* (cathelicidin LL-37) in wound healing, as has been previously reported.[11–14] The stronger and more prolonged response obtained with the presence of 4HB can potentially provide for improved clinical outcomes [46]

The phenotypic profile of macrophages within the early period postimplantation (i.e., 7–14 days) has been shown to be predictive and determinant of downstream clinical outcome (i.e., site appropriate tissue remodeling vs. fibrotic tissue).[47] Using a rat abdominal bilateral partial thickness defect to evaluate the host tissue response to implanted surgical meshes, we have previously shown that macrophages show an increased ratio of proremodeling (M2-like) macrophages to

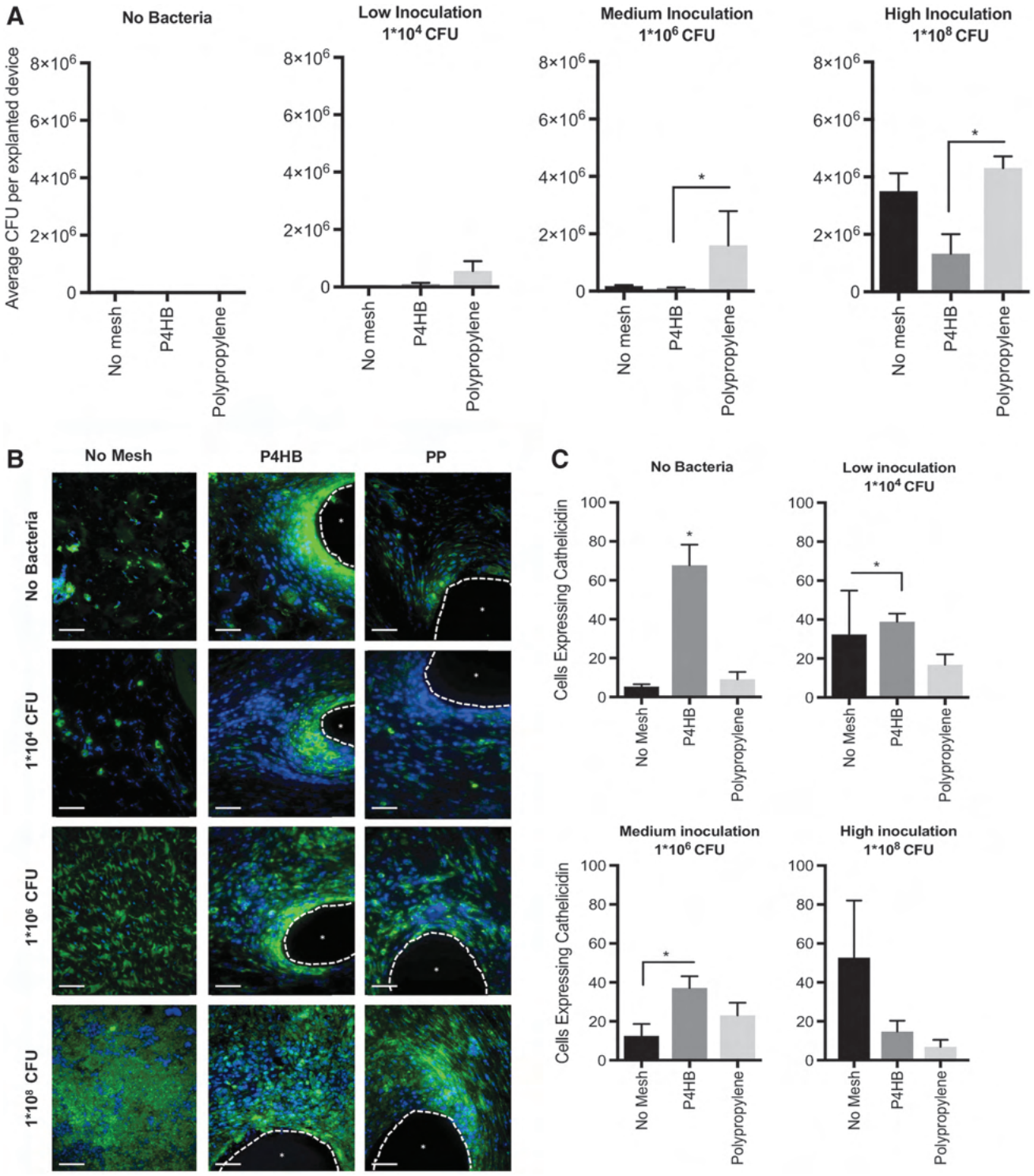

FIG. 7. Resistance of implanted meshes to deliberate bacterial contamination. **(A)** Quantification of colonizing *S. aureus* in explanted specimens 14 days postimplantation. Significance represents differences in the number of CFU between the mesh materials at each inoculation level. Fiber location is delineated by a *dotted line* and an *asterisk*. Scale bar 50 μm. Values: mean ± SEM, $N = 6$ biological replicates, technical triplicates, $^*p < 0.05$. **(B)** Representative images of cathelicidin LL-37 expressed around the fibers of P4HB and PP at each bacterial inoculation level. **(C)** Quantification of cells expressing cathelicidin LL-37. Value: mean ± SEM, $N = 4$ biological replicates, technical triplicates, $^*p < 0.05$.

proinflammatory (M1-like) macrophages at early time points postimplantation of a P4HB surgical mesh, compared with the marked proinflammatory response seen with synthetic surgical meshes.

The ratio of M2-like: M1-like macrophages interacting with P4HB was also associated with a decreased number of foreign body giant cells.[46] The findings are consistent with preclinical[48] and clinical[49] data showing favorable long-term outcomes. In addition, this study showed the ability of 4HB to immunomodulate the *in vitro* response of proinflammatory macrophages by increasing the expression of proremodeling markers such as Arginase1 and Fizz1 when compared with nonstimulated macrophages.[46]

Current approaches to control biomaterial-associated bacterial infections involve the use of antimicrobial agents that rely on proliferative stages of colonizing bacteria, rendering these approaches ineffective in biofilms. Bacterial resistance to most common antimicrobial agents has evolved, limiting the number of therapeutic options and increasing the burden of infected patients. Considering both nonbiomaterial- and biomaterial-related infections, it is estimated that by 2050 resistant bacterial infections will affect >10 million people per year worldwide, if more effective strategies are not identified.[50]

The recognition that AMPs kill bacteria through mechanisms that do not depend on the metabolic activity of the pathogens provides an effective mode of protection against them without the risk of developing resistance. The exogenous administration of AMP is being explored[13]; however, this mode of use raises questions regarding the stability of the peptides and the methods for delivery, and provides only temporary protection. This study investigated an alternative approach that enhances endogenous antimicrobial activity of the immune system through increased production of AMPs by host cells, thus generating a stronger and more prolonged response.

There are several limitations to this study. Expression of the AMP cathelicidin LL-37 was evaluated by transcriptional activation of the *cramp* gene and protein expression on stimulated murine bone marrow-derived macrophages. Additional characterization of the macrophage phenotypic profile induced by the evaluated SCFAs, quantification of secreted AMPs into the media, and identification of the mechanisms driving the expression of these AMPs is warranted in future studies.

Acknowledgments

C.P.M. was supported by the Colciencias-Fulbright Scholarship and the Tuition Remission Fellowship (TRF) from The Center for Latin American Studies (CLAS), University of Pittsburgh. The authors thank Lori Walton from the Histology Center at the McGowan Institute for Regenerative Medicine for histological section preparation. Partial funding of this study was provided by Becton, Dickinson and Company/CR Bard, Inc.

Disclosure Statement

No competing financial interests exist.

Supplementary Material

Supplementary Table S1
Supplementary Figure S1
Supplementary Figure S2

References

1. Daghighi, S., Sjollema, J., van der Mei, H.C., Busscher, H.J., and Rochford, E.T. Infection resistance of degradable versus non-degradable biomaterials: an assessment of the potential mechanisms. Biomaterials **34,** 8013, 2013.
2. Busscher, H.J., van der Mei, H.C., Subbiahdoss, G., *et al.* Biomaterial-associated infection: locating the finish line in the race for the surface. Sci Transl Med **4,** 153rv10, 2012.
3. Zaat, S., Broekhuizen, C., and Riool, M. Host tissue as a niche for biomaterial-associated infection. Future Microbiol **5,** 1149, 2010.
4. Batoni, G., Maisetta, G., and Esin, S. Antimicrobial peptides and their interaction with biofilms of medically relevant bacteria. Biochim Biophys Acta **1858,** 1044, 2016.
5. Duplantier, A.J., and van Hoek, M.L. The human cathelicidin antimicrobial peptide ll-37 as a potential treatment for polymicrobial infected wounds. Front Immunol **4,** 143, 2013.
6. McCloskey, A.P., Gilmore, B.F., and Laverty, G. Evolution of antimicrobial peptides to self-assembled peptides for biomaterial applications. Pathogens **3,** 791, 2014.
7. Kasetty, G., Kalle, M., Morgelin, M., Brune, J.C., and Schmidtchen, A. Anti-endotoxic and antibacterial effects of a dermal substitute coated with host defense peptides. Biomaterials **53,** 415, 2015.
8. Zasloff, M. Inducing endogenous antimicrobial peptides to battle infections. Proc Natl Acad Sci U S A **103,** 8913, 2006.
9. Vandamme, D., Landuyt, B., Luyten, W., and Schoofs, L. A comprehensive summary of LL-37, the factotum human cathelicidin peptide. Cell Immunol **280,** 22, 2012.
10. Wang, G. Human antimicrobial peptides and proteins. Pharmaceuticals **7,** 545, 2014.
11. Ramos, R., Silva, J.P., Rodrigues, A.C., *et al.* Wound healing activity of the human antimicrobial peptide LL37. Peptides **32,** 1469, 2011.
12. Winter, J., and Wenghoefer, M. Human defensins: potential tools for clinical applications. Polymers **4,** 691, 2012.
13. Silva, J.P., Dhall, S., Garcia, M., *et al.* Improved burn wound healing by the antimicrobial peptide LLKKK18 released from conjugates with dextrin embedded in a carbopol gel. Acta Biomater **26,** 249, 2015.
14. Koczulla, R., von Degenfeld, G., Kupatt, C., *et al.* An angiogenic role for the human peptide antibiotic LL-37/hCAP-18. J Clin Invest **111,** 1665, 2003.
15. Sun, M., Wu, W., Liu, Z., and Cong, Y. Microbiota metabolite short chain fatty acids, GPCR, and inflammatory bowel diseases. J Gastroenterol **52,** 1, 2017.
16. Donohoe, D.R., Collins, L.B., Wali, A., Bigler, R., Sun, W., and Bultman, S.J. The Warburg effect dictates the mechanism of butyrate-mediated histone acetylation and cell proliferation. Mol Cell **48,** 612, 2012.
17. Ji, J., Shu, D., Zheng, M., *et al.* Microbial metabolite butyrate facilitates M2 macrophage polarization and function. Sci Rep **6,** 24838, 2016.
18. Park, J.S., Lee, E.J., Lee, J.C., Kim, W.K., and Kim, H.S. Anti-inflammatory effects of short chain fatty acids in IFN-gamma-stimulated RAW 264.7 murine macrophage cells: involvement of NF-kappaB and ERK signaling pathways. Int Immunopharmacol **7,** 70, 2007.
19. Owen, O.E., Morgan, A.P., Kemp, H.G., Sullivan, J.M., Herrera, M.G., and Cahill, G.F., Jr. Brain metabolism during fasting. J Clin Invest **46,** 1589, 1967.
20. Nelson, T., Kaufman, E., Kline, J., and Sokoloff, L. The extraneural distribution of g-hydroxybutyrate. J Neurochem **37,** 1345, 1981.

21. Gall, W.E., Beebe, K., Lawton, K.A., *et al.* alpha-hydroxybutyrate is an early biomarker of insulin resistance and glucose intolerance in a nondiabetic population. PLoS One **5,** e10883, 2010.
22. Kimura, I., Inoue, D., Maeda, T., *et al.* Short-chain fatty acids and ketones directly regulate sympathetic nervous system via G protein-coupled receptor 41 (GPR41). Proc Natl Acad Sci U S A **108,** 8030, 2011.
23. Mamelak, M. Alzheimer's disease, oxidative stress and gammahydroxybutyrate. Neurobiol Aging **28,** 1340, 2007.
24. Chen, G.Q., and Wu, Q. The application of polyhydroxyalkanoates as tissue engineering materials. Biomaterials **26,** 6565, 2005.
25. Williams, S.F., Rizk, S., and Martin, D.P. Poly-4-hydroxybutyrate (P4HB): a new generation of resorbable medical devices for tissue repair and regeneration. Biomed Tech (Berl) **58,** 439, 2013.
26. Valentin, J.E., Badylak, J.S., McCabe, G.P., and Badylak, S.F. Extracellular matrix bioscaffolds for orthopaedic applications. A comparative histologic study. J Bone Joint Surg Am **88,** 2673, 2006.
27. Sicari, B., Turner, N., and Badylak, S.F. An in vivo model system for evaluation of the host response to biomaterials. Methods Mol Biol **1037,** 3, 2013.
28. Bellows, C.F., Wheatley, B.M., Moroz, K., Rosales, S.C., and Morici, L.A. The effect of bacterial infection on the biomechanical properties of biological mesh in a rat model. PLoS One **6,** e21228, 2011.
29. Englen, M.D., Valdez, Y.E., Lehnert, N.M., and Lehnert, B.E. Granulocyte/macrophage colony-stimulating factor is expressed and secreted in cultures of murine L929 cells. J Immunol Methods **184,** 281, 1995.
30. Sicari, B.M., Dziki, J.L., Siu, B.F., Medberry, C.J., Dearth, C.L., and Badylak, S.F. The promotion of a constructive macrophage phenotype by solubilized extracellular matrix. Biomaterials **35,** 8605, 2014.
31. Lee, P.H., Ohtake, T., Zaiou, M., *et al.* Expression of an additional cathelicidin antimicrobial peptide protects against bacterial skin infection. Proc Natl Acad Sci U S A **102,** 3750, 2005.
32. Chong, K.T., Thangavel, R.R., and Tang, X. Enhanced expression of murine beta-defensins (MBD-1, −2,−3, and −4) in upper and lower airway mucosa of influenza virus infected mice. Virology **380,** 136, 2008.
33. van der Does, A.M., Kenne, E., Koppelaar, E., Agerberth, B., and Lindbom, L. Vitamin D(3) and phenylbutyrate promote development of a human dendritic cell subset displaying enhanced antimicrobial properties. J Leukocyte Biol **95,** 883, 2014.
34. Cleries, R., Galvez, J., Espino, M., Ribes, J., Nunes, V., and de Heredia, M.L. BootstRatio: a web-based statistical analysis of fold-change in qPCR and RT-qPCR data using resampling methods. Comput Biol Med **42,** 438, 2012.
35. Newman, J.C., and Verdin, E. beta-hydroxybutyrate: much more than a metabolite. Diabetes Res Clin Pract **106,** 173, 2014.
36. Xiong, H., Guo, B., Gan, Z., *et al.* Butyrate upregulates endogenous host defense peptides to enhance disease resistance in piglets via histone deacetylase inhibition. Sci Rep **6,** 27070, 2016.
37. Tan, J., McKenzie, C., Potamitis, M., Thorburn, A.N., Mackay, C.R., and Macia, L. The role of short-chain fatty acids in health and disease. Adv Immunol **121,** 91, 2014.
38. Mottamal, M., Zheng, S., Huang, T.L., and Wang, G. Histone deacetylase inhibitors in clinical studies as templates for new anticancer agents. Molecules **20,** 3898, 2015.
39. Shimazu, T., Hirschey, M.D., Newman, J., *et al.* Suppression of oxidative stress by beta-hydroxybutyrate, an endogenous histone deacetylase inhibitor. Science **339,** 211, 2013.
40. Klein, C., Kemmel, V., Taleb, O., Aunis, D., and Maitre, M. Pharmacological doses of gamma-hydroxybutyrate (GHB) potentiate histone acetylation in the rat brain by histone deacetylase inhibition. Neuropharmacology 57, 137, 2009.
41. Bay, T., Eghorn, L.F., Klein, A.B., and Wellendorph, P. GHB receptor targets in the CNS: focus on high-affinity binding sites. Biochem Pharmacol **87,** 220, 2014.
42. Steinmann, J., Halldorsson, S., Agerberth, B., and Gudmundsson, G.H. Phenylbutyrate induces antimicrobial peptide expression. Antimicrob Agents Chemother **53,** 5127, 2009.
43. Sarker, P., Ahmed, S., Tiash, S., *et al.* Phenylbutyrate counteracts Shigella mediated downregulation of cathelicidin in rabbit lung and intestinal epithelia: a potential therapeutic strategy. PLoS One **6,** e20637, 2011.
44. Zeng, X., Sunkara, L.T., Jiang, W., *et al.* Induction of porcine host defense peptide gene expression by short-chain fatty acids and their analogs. PLoS One **8,** e72922, 2013.
45. Zhang, G.F., Sadhukhan, S., Ibarra, R.A., *et al.* Metabolism of gamma-hydroxybutyrate in perfused rat livers. Biochem J **444,** 333, 2012.
46. Pineda Molina, C., Giglio, R.M., Gandhi, R.M., *et al.* Comparison of the host macrophage response to synthetic and biologic surgical meshes used for ventral hernia repair. J Immunol Regen Med **3,** 13, 2019.
47. Brown, B.N., Londono, R., Tottey, S., *et al.* Macrophage phenotype as a predictor of constructive remodeling following the implantation of biologically derived surgical mesh materials. Acta Biomater **8,** 978, 2012.
48. Deeken, C.R., and Matthews, B.D. Characterization of the mechanical strength, resorption properties, and histologic characteristics of a fully absorbable material (poly-4-hydroxybutyrate-PHASIX mesh) in a porcine model of hernia repair. ISRN Surg **2013,** 238067, 2013.
49. Roth, J.S., Anthone, G.J., Selzer, D.J., *et al.* Prospective evaluation of poly-4-hydroxybutyrate mesh in CDC class I/high-risk ventral and incisional hernia repair: 18-month follow-up. Surg Endosc **32,** 1929, 2018.
50. O'Neill, J. Tackling Drug-Resistant Infections Globally: Final Report and Recommendations. London, United Kingdom: Review on Antimicrobial Resistance (AMR), 2016.

Address correspondence to:
Stephen F. Badylak, DVM, PhD, MD
McGowan Institute for Regenerative Medicine
University of Pittsburgh
450 Technology Drive, Suite 300
Pittsburgh, PA 15219

E-mail: badylaks@upmc.edu

Received: December 23, 2018
Accepted: March 26, 2019
Online Publication Date: May 8, 2019